# Point spread functions for a small gamma camera with pinhole collimator

LIU Shi-Tao, XU Zi-Zong, WANG Zhao-Min, XU Shen-Bo

*(Department of Modern Physics, University of Science and Technology of China, Hefei 230027)*

**Abstract** A set of point spread functions (PSF) has been obtained by means of Monte-Carlo simulation for a small gamma camera with a pinhole collimator of various hole diameters. The FOV (field of view) of the camera is expended from 45 mm to 70 mm in diameter. The position dependence of the variances of PSF is presented, and the acceptance for the 140 keV gamma rays is explored. A phantom of 70 mm in diameter was experimentally imaged in the camera with effective FOV of only 45 mm in diameter.

**Keywords** Gamma camera, Point spread function, Pinhole collimator, Monte-Carlo simulation

**CLC numbers** TL812, R730.44

## 1 Introduction

Anger gamma camera[1] with a planar scintillator coupled to an array of photo-multipliers has been widely used in clinical diagnosis. But large size and weight and large dead zone of Anger camera make it difficult to operate for some applications, such as scinti-mammography and radio-guided surgery. There are many demands on a compact gamma camera for a single organ imaging or a gamma ray telescope[2] in both medical and astrophysical fields. A small gamma camera consisting of a planar crystal, coupled with PSPMT (position-sensitive photo-multiplier tube) has been explored.[3-5] It could provide better intrinsic spatial resolution and was suitable to the flexible applications. But the relative small field of view (FOV) was a limit for some applications. For example, a portable gamma camera using a Hamamashu-R2486 tube has only $\phi$45 mm effective FOV when a parallel collimator is matched with it. It is not enough to make a whole organ, like thyroid and breast, imaged. A pinhole instead of parallel collimator could expand FOV of gamma camera at the expense of its space resolution in the object plane. A pinhole collimator is usually made of a cylindrical lead block with a shape like Fig.1, very different from that of the optical pinhole imaging which contains a sheet of black paper with a small hole. Gamma ray of energies like 140 keV could pass even through the lead pinhole collimator from different incident directions with very different probabilities. It means that the gamma rays see a diffused hole instead of a hole with a sharp edge. Monte Carlo (MC) simulation is a right way to study the properties

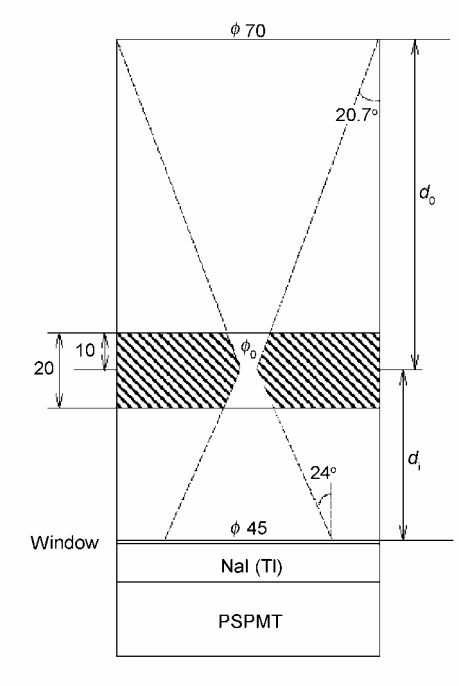


**Fig.1** A schematic diagram of the compact gamma camera with a pinhole collimator(mm).

Supported by the National Natural Science Foundation of China (10275063)
Received date: 2002-05-31

of such kind of collimator. As the acceptance and the point spread function (PSF) obtained based on the MC simulation could really reflect performance of the collimator, parameters of the acceptance and PSF are very useful for image reconstruction and correction in future application of the camera.

## 2 Description of the simulation

The simulation is based on the GEANT3 program library developed at CERN. The geometric description of the pinhole collimator is shown in Fig.1. This is a cylindrical lead block with two coaxial cone cavities from both top and bottom sides. The up-cone has a little bit less half-cone angle than the one of the down-cone and the overlap of the two cones' tips is adjusted to have a proper diameter of passing through the hole: $\phi_0$. So the gamma rays from the object along the surface of the up-cone, down through the hole, can reach the image plane without additional absorption. To assemble the collimator coaxial with the PSPMT camera we adjusted the image distance $d_i$ (the distance between the center of hole and the middle of entrance window of the planar scintillator) to 46 mm and make the image field with a diameter of 45 mm. Assuming the distance between the center of hole and the object plane as $d_0$, the linear amplification will equal $22.5/(d_0 \mathrm{tg}20.7^{\circ}+0.5\phi_0)$. For different $d_0$, the camera will have different amplification power. This zoom function makes this compact camera be able to work either with large FOV/ worse space resolution or with small FOV/ better space resolution in the object plane.

The geometric parameters are described in Fig.1, The lead pinhole collimator was machined with 20 mm high and 84 mm in diameter. The half angles of up-cone and down-cone are 20.7o and 24o, respectively. A planar NaI(Tl) crystal of $\phi$100 mm × 10 mm was coupled with the PSPMT R2486 which was reading the barycenter of the distribution of scintillating photons produced from a hit event of gamma rays. The MC simulation starts with a point source of gamma ray of energy 140keV on the object plane of $d_0$ = 83 mm, located at ($X$, $Y$)o. Then succeed the following procedures: (1) generate a gamma ray at random; (2) justify whether the ray is going through the hole (gamma ray through the lead material without absorption is also included), if it does not penetrate through the hole, add 1 in the counter SUM, and regenerate a new event; (3) trace the gamma ray incident on the crystal; if the gamma ray escapes from the crystal, add 1 to the counter SUM; (4) if the photoelectric absorption happens in the crystal, record the interaction position ($x$, $y$), call the PSFG which is the spread of the barycenter of the distribution of the scintillating photons produced by one interaction gamma ray in the position ($x$, $y$);[6,7] sampling according to the probability distribution PSFG ($x$, $y$) make the final image point $(X, Y)^I$ recorded and add 1 to both counters ACCE and SUM; when the SUM counter has a number of $10^6$, stop this sampling and move the point source to the next position on the object plane; (5) the acceptance will be calculated with the number in the ACCE divided by the number in the SUM; do the histogram of data set of $(X, Y)^I$; the PSF system with the effect of the pinhole collimator is obtained. Fig.2 shows a typical PSF.

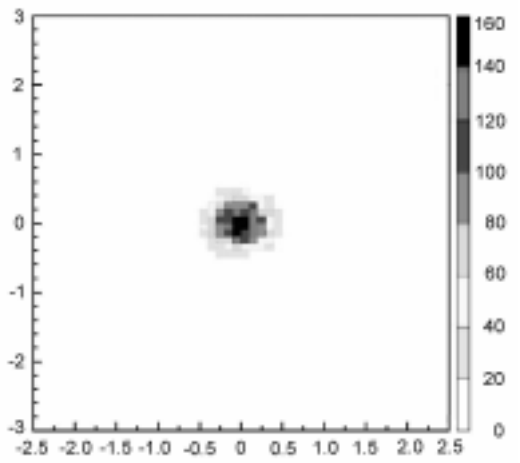


**Fig.2** Typical PSF with the point source located at the center (cm).

## 3 Results and Discussion

### 3.1 Position response and space resolution

The point gamma source in the object plane coaxial with the camera moves step by step (step length of 3 mm) from the center along the radial direction and generates 12 sets of the PSF system for various sizes of pinhole $\phi_0$ = 3, 4, 5 mm, like Fig.2. Fit the PSF system with Gaussian distribution one by one. The position of the barycenter and the variance of the distribution are the image position and the space resolution respectively for a given object position of the

point source. Fig.3 shows the position response of the camera with various diameters of pinhole collimator (Phy3, Phy4 and Phy5 in the plot present data produced in different pinhole diameters 3, 4 and 5 mm, respectively). The property of inverse imaging is indicated from the opposite sign between the source and image coordinates and the minified image was seen from the absolute values of the $X$ and $Y$ coordinates. The effects of image shrinkage are reflected apparently both in non-linear position response and in resolution's improvement in the periphery. The larger diameter of the holes is, the more serious effects of shrinkage happen. Ref.[8] has explained the mechanism causing this shrinkage.

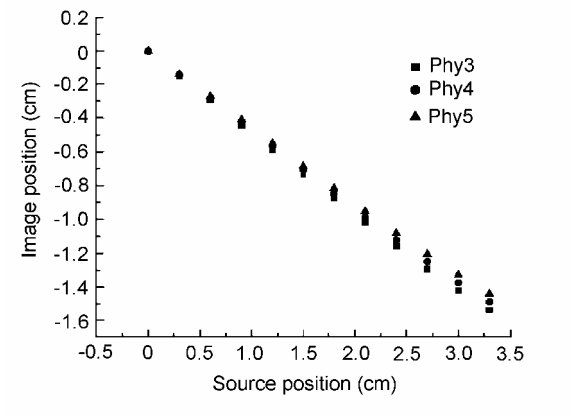


**Fig.3** Position response for various pinhole diameters.

Fig.4 shows the source position dependence of the space resolution in the image plane. The average space resolution over the radial 12 positions are 2.8 mm, 3.5 mm and 4.1 mm for the hole diameters of 3, 4 and 5 mm, respectively. It is apparent that the space resolution is determined mainly by the hole diameters.

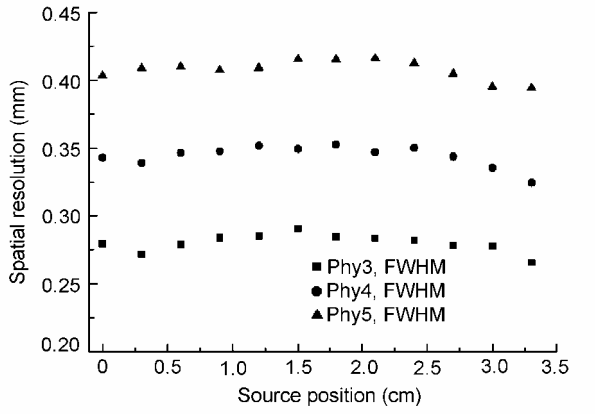


**Fig.4** Space resolution for various pinhole diameters.

### 3.2 Acceptance of the camera

The smaller hole is, the higher space resolution will be. The choice of hole diameter should be balanced between acceptance and resolution. The dependence of acceptance efficiency on hole diameter in various source positions is shown in Fig.5. The acceptance has a little decrease from the center to the periphery of the object plane. The average acceptances over the 12 source positions are 0.04%, 0.06% and 0.09% for the hole diameters of 3, 4 and 5 mm, respectively. A pinhole collimator has been manufactured with $\phi_0$ = 4 mm. Its acceptance (0.06%) is comparable with our parallel collimator.

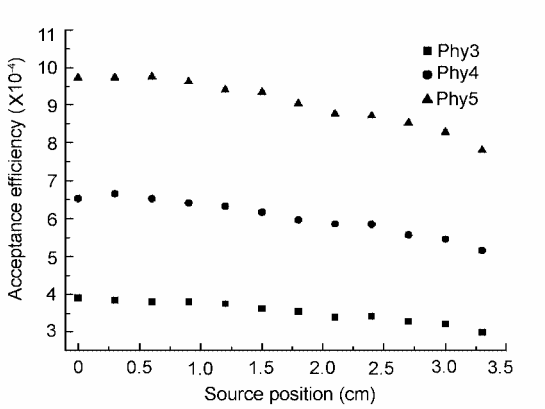


**Fig.5** The hole diameter dependence of acceptance in various source positions.

## 4 The phantom image of the camera

In order to test properties of this compact camera with the manufactured pinhole collimator, a glass phantom was made. The phantom is 70 mm in diameter with 4 bubbles in its cavity. The cavity is filled with lower specific activity $^{99m}$Tc. The four bubbles are 6 mm (1), 5 mm (2), 4 mm (3) and 4 mm (4) in diameter, respectively. The hot bubbles 1 and 2 are 40 mm away and filled with 10 times higher specific activity of $^{99m}$Tc. The cold bubbles 3 and 4 are 35 mm away and empty. We locate the phantom at the position of $d_0$ = 80 mm in the experiment. Fig.6 shows the image of this phantom. The two hot bubbles are clearly seen and the two cold bubbles can be identified though it is not seen so clearly.

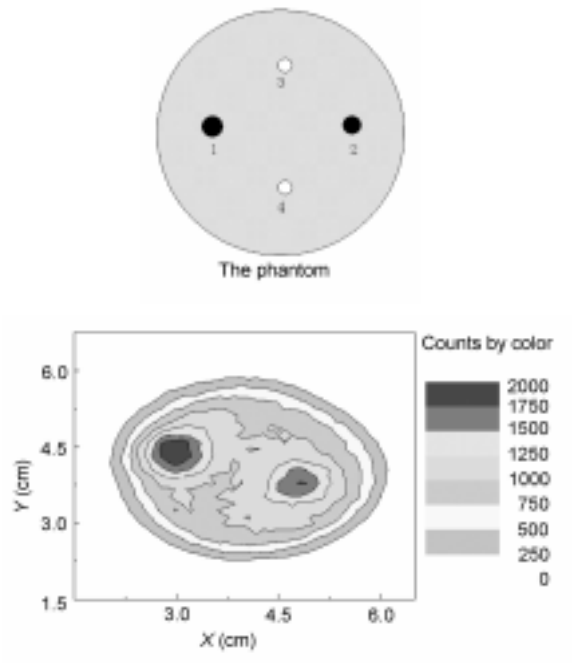


**Fig.6** A phantom and its image.

## 5 Conclusion

A compact gamma camera has adjustable FOV owing to the pinhole collimator. The Monte Carlo simulation suggests that the camera with pinhole of 3, 4 and 5 mm diameter has its position resolution of 2.8 mm, 3.5 mm and 4.1 mm and its acceptance of 0.04%, 0.06% and 0.09%, respectively. The gamma camera is able to expand the camera FOV from $\phi$45 mm to $\phi$70 mm. A phantom of 70 mm in diameter is well imaged in the image plane with only 45 mm effective diameter. A series of the PSF system and the acceptance data sets of the camera obtained from the Monte Carlo simulation will be useful in the future image processing.

## Acknowledgement

We greatly appreciated the support to the experiment from the Division of Nuclear Medicine of the Anhui Hospital.

## References

1 Bird A J, Ramsden D. Nucl Instr Meth, 1990, A**299**: 480-483

2 Mandrou P. Adv Space Res, 1984, **3**: 525

3 Clancy R L, Thompson C J, Robar J L *et al*. IEEE Trans Nucl Sci, 1997, **44**(3): 494-498

4 Smith L E, He Z, Wehe D K *et al*. IEEE Trans Nucl Sci, 1998, **45**(3): 963-969

5 Guru S V, He Z, Ferreria J C *et al*. Nucl Instr Meth, 1994, A**353**: 328-333

6 Zeng H N, Xu Z Z, Wang Z M *et al*. High Energy Phys Nucl Phys (in Chinese), 2000, **24**(2): 166-171

7 Zeng H N, Xu Z Z, Wang Z M *et al*. High Energy Phys Nucl Phys (in Chinese), 2000, **24**(11): 1050-1054

8 Zeng H N, Xu S B, Liu S T *et al*. Acta Photonica Sin, 2001, **30**(11): 1321-1324